Eye and Brain

Dovepress
Taylor & Francis Group

Open Access Full Text Article

ORIGINAL RESEARCH

A Novel Retinal Nerve Fiber Layer Biomarker of Amyotrophic Lateral Sclerosis (ALS) Identified Using Longitudinal in vivo Ocular Imaging

Farbod Khorrami[1,2], Neeru Gupta[1–5], Xun Zhou[1], You Liang[6], Yeni H Yucel[1–4,7–9]

[1]Keenan Research Centre for Biomedical Science, Li Ka Shing Knowledge Institute, St. Michael's Hospital, Toronto, ON, Canada; [2]Department of Laboratory Medicine and Pathobiology, Temerty Faculty of Medicine, University of Toronto, Toronto, ON, Canada; [3]Department of Ophthalmology and Vision Sciences, Temerty Faculty of Medicine, University of Toronto, Toronto, ON, Canada; [4]Department of Ophthalmology and Visual Sciences, University of British Columbia, Vancouver, BC, Canada; [5]School of Population and Public Health, Faculty of Medicine, University of British Columbia, Vancouver, BC, Canada; [6]Department of Mathematics, Toronto Metropolitan University, Toronto, ON, Canada; [7]Department of Physics, Faculty of Science, Toronto Metropolitan University, Toronto, ON, Canada; [8]Institute of Biomedical Engineering, Science and Technology (iBEST), St. Michael's Hospital, Toronto Metropolitan University, Toronto, ON, Canada; [9]Department of Mechanical Engineering, Faculty of Engineering and Architectural Science, Toronto Metropolitan University, Toronto, ON, Canada

Correspondence: Yeni H Yucel, Ophthalmic Pathology Laboratory, Temerty Faculty of Medicine, University of Toronto, Keenan Research Centre for Biomedical Science, St. Michael's Hospital, Unity Health Toronto, 30 Bond Street, 209 LKSKI, Room 409, Toronto, ON, M5B 1W8, Canada, Tel +1 416 864-6060 - Ext: 77594, Email yeni.yucel@unityhealth.to

Purpose: Like motor neurons, retinal ganglion cells (RGCs) have long axons and high metabolic demands, making them vulnerable to disruption of axonal transport. Unlike motor neurons, the RGC axons are accessible to high-resolution non-invasive optical imaging in their intraocular portion. A non-invasive in vivo retinal imaging biomarker can be valuable for amyotrophic lateral sclerosis (ALS) diagnosis and monitoring. We aim to assess the presence of inner retinal pathology in a mouse model of ALS and its possible progression with age.

Methods: Transgenic SOD1G93A mice (n=8, 4M/4F) and age-matched controls (n=8, 4M/4F) underwent in vivo retinal imaging with confocal scanning laser ophthalmoscopy (cSLO) coupled with optical coherence tomography (OCT) at 20 weeks of age. Another group of SOD1G93A mice (n=20, 6M/14F) and age-matched controls (n=20, 6M/14F) underwent longitudinal in vivo retinal imaging with the same device. Each retinal imaging session included infrared reflectance (IR) and blue reflectance (BR) cSLO coupled with OCT. Hyperreflective puncta located in the retinal nerve fiber layer (RNFL) were counted in a blinded fashion in ALS and control mice. The number of puncta at 20 weeks of age in ALS mice was compared with controls using Wilcoxon test. The rates of increase of puncta number were analyzed using a Generalized Linear Mixed-Effect Model (GLMM) for genotype, time, and sex.

Results: IR-cSLO coupled with OCT revealed hyperreflective puncta located in the RNFL of ALS mice. IR-cSLO fundus imaging at the age of 20 weeks showed ALS mice had significantly higher number of puncta compared to controls (2.1±2.3 vs 0.5±0.8; (mean ±SD), respectively, p=0.036). GLMM analysis showed both ALS mutation and age were significantly associated with the rate of increase of puncta number (p=0.000232 and p=0.000366, respectively). In addition, female ALS mice had a steeper increase of puncta compared to male ALS mice (0.21±0.04 log number puncta/week vs 0.16±0.04, respectively; p=0.037).

Conclusion: Our findings demonstrate distinct inner retinal nerve fiber layer pathology, detected using cSLO coupled with OCT, which worsens over time. These findings support the potential of retinal imaging as a translationally relevant, non-invasive biomarker for ALS diagnosis or disease monitoring in humans.

Keywords: amyotrophic lateral sclerosis, retinal nerve fiber layer, superoxide dismutase, mouse, eye imaging, optical coherence tomography, sex, spheroids, pathology, hyperreflective, puncta

Introduction

Amyotrophic lateral sclerosis (ALS) is an incurable and rapidly progressive neurodegenerative disease that primarily affects the motor neurons.[1] ALS shows heterogeneity in its clinical features and heredity.[2] Clinical phenotypes with

Received: 8 January 2025
Accepted: 20 June 2025
Published: 2 July 2025

motor deficits vary depending on the site of onset and rate of progression.[3] Cognitive phenotypes and various degrees of frontotemporal dementia are also present in up to half of ALS patients.[4] ALS shows marked sex-dependent differences, with male patients having higher prevalence,[5] earlier onset,[6] and faster progression[7] than female patients.[8] Approximately 10% of ALS cases have a family history; the rest occur sporadically.[9] Several genetic mutations have been linked to ALS, with approximately 20% of patients with familial ALS having superoxide dismutase 1 (*SOD1*) mutations.[10]

The heterogeneity of ALS makes diagnosis and patient management challenging and poses difficulties for clinical trials. Therefore, the use of biomarkers is critical for both patient care and clinical trials. The current ALS biomarkers are based on clinical examination, neuroimaging, biochemical assays of blood and cerebrospinal fluid, and electrophysiology.[11–14] There is an urgent need for additional non-invasive, repeatable, and biologically plausible biomarkers to detect and monitor ALS phenotypes over time, to stratify patients, and to assess therapeutic responses in clinical trials.[15] A promising avenue for the development of novel biomarkers is targeting the mechanisms implicated in ALS pathogenesis and progression.

ALS involves complex pathobiological mechanisms, with disruption of axonal transport being a major mechanism.[16,17] Axonal transport is an active process; cargoes are moved by motor proteins along microtubules between the cell body and the axon terminal.[18,19] Neurons with long axons, such as motor neurons, are particularly susceptible to disruption of axonal transport, leading to degeneration and accumulations of cargoes in the axons.[20] Axonal spheroids in the motor neurons represent a neuropathological hallmark of ALS; they are composed of proteins such as neurofilaments (NFs), and organelles.[21–23] Axonal spheroids are a potential target for developing imaging biomarkers for ALS. However, current neuroimaging techniques, such as MRI, do not have the spatial resolution to detect the microscopic axonal spheroids in motor neurons in the brain and spinal cord.

Clinical optical imaging modalities of the retina with higher spatial resolution enable the imaging of retinal ganglion cell (RGC) axons that convey the visual information from the eye to the central visual centers.[24] Similar to motor neurons, RGCs have long axons[25] and high metabolic demands, making them susceptible to disruption of axonal transport.[26] Clinical retinal imaging modalities, such as optical coherence tomography (OCT), have been used to assess retinal layers and blood vessels. The innermost layer, the retinal nerve fiber layer (RNFL), contains the RGC axons and its thickness is measured to assess retinal changes in glaucoma and some neurodegenerative diseases.[27] Previous OCT studies of RNFL in ALS patients showed discordant results.[28] In some cross-sectional studies, peripapillary RNFL was thinner in ALS group compared to control group[29,30] while in other studies, no differences were detected between ALS and control groups.[31,32] A follow-up study showed a correlation between peripapillary RNFL thinning with ALS clinical severity.[33] Furthermore, OCT studies of retinal vasculature described significant vascular changes in ALS,[34] and some of the ocular vascular changes correlated with ALS aggressiveness.[35] We have previously identified axonal spheroids in RGC axons within the RNFL in post-mortem retina sections from sporadic ALS patients.[36] However, it is not yet known whether clinical eye imaging modalities can detect in vivo retinal phenotypes in ALS.

In this paper, we aim to demonstrate that retinal phenotypes in ALS can be detected in vivo using clinical eye imaging devices. Although retinal imaging findings in a mouse model of ALS may point to a potential biomarker for human ALS diagnostics and monitoring, careful consideration of which retinal features are similar between mice and humans, and which are different, is needed. Both mouse and human share a multilayered organization of retinas, consisting of three cellular layers, two synaptic layers, and an axonal layer. Notably, mice have a smaller retina, fewer RGCs, and a lower RGC density than humans.[37]

We imaged the retina of ALS mice and controls with confocal scanning laser ophthalmoscope (cSLO) coupled with OCT. The retinal phenotyping study targeted on the RNFL containing of axons of RGCs in a widely used mouse model of ALS, transgenic mice with a mutated human *SOD1* gene (*SOD1G93A*). This mouse model exhibits axonal spheroids in motor neurons and has motor deficits similar to ALS patients.[38] We hypothesize that the SOD1 ALS mouse model exhibits a progressive retinal phenotype, marked by an increase in hyperreflective puncta over time, and that this progression differs by sex.

Materials and Methods

Animal Subjects and Clinical Monitoring

The study was designed in accordance with guidelines from the Association for Research in Vision and Ophthalmology (ARVO) and was approved by the Unity Health Toronto Animal Care Committee. Transgenic mice with a mutated human *SOD1* gene (*SOD1G93A*) associated with ALS[38] (strain number: 004435, 2 months old, n = 28, 10M/18F), and age-matched controls (C57BL/6J, n = 28, 10M/18F) were used (Jackson Laboratories, Bar Harbor, ME, USA). Mice were group-housed (4 of the same sex per cage) in the Animal Care Facility of the Keenan Research Centre for Biomedical Science, St. Michael's Hospital, Unity Health Toronto, on a 12-hour light-dark cycle, with unrestricted access to food and water. Body weight measurement and motor assessment were performed once a week. Motor assessment monitoring included hindlimb extension reflex and tremor using a scoring system on a scale from 1 to 4 (1 being the lowest and 4 being the highest rating) modified from previous studies.[39,40] The data collection and analysis were performed in a blinded fashion.

In vivo Retinal Imaging

In vivo retinal imaging was performed using a cSLO combined with optical coherence tomography (OCT) (Spectralis HRA + OCT, Heidelberg Engineering Inc., Heidelberg, Germany) as previously described.[41] To prevent corneal dehydration during the imaging session performed under general anesthesia with 2% isoflurane inhalation, 1 mL of saline (0.9% NaCl Injection, USP, Baxter Corporation, Mississauga, Canada) was injected subcutaneously (25G x 5/8" BD Eclipse needle and BD Slip Tip Sterile Syringe) and a custom-made contact lens (BOZR 1.70, DIAM 3.20, and PWR PLANO, Cantor and Nissel Ltd, Northamptonshire, United Kingdom) was placed on the cornea.[42] cSLO fundus imaging modalities included Infrared Reflectance (IR, 815 nm), Blue Reflectance (BR, 486 nm), Green Reflectance (GR, 514 nm), and autofluorescence (AF, 486 nm and 786 nm). Hyperreflective profiles were detected in ALS mice using the IR-cSLO modality. B-scans of the OCT image of IR-hyperreflective profiles were used to determine their location within the RNFL. Hyperreflective IR-puncta (IR-puncta), defined as IR-hyperreflective profiles localized to the RNFL, were counted in a blinded fashion, and profiles that were not localized to the RNFL were excluded. For the first set of experiments, the results of the retinal imaging performed at 20 weeks were used to determine if there are any differences in retinal phenotypes between ALS (n = 8, 4M/4F) and control (n = 8, 4M/4F) mice at the later stage of the disease. For the second set of experiments, longitudinal eye imaging of ALS (n=20, 6M/14F) and control mice (n=20, 6M/14F) was conducted once every two weeks from 9 weeks of age to 20 weeks. The retinal imaging started in mice after 9 weeks of age because the eye parameters relevant for eye imaging, such as axial length, lens thickness, anterior chamber depth and corneal thickness that are important for the optics of the eye during imaging, are stable after 8 weeks.[43,44] The last imaging session was performed at 20 weeks of age, before advanced clinical signs. Motor signs were monitored by tremor and hindlimb extension reflex scores for the endpoint as established by the Unity Health Toronto Animal Care Committee for humane treatment of animal subjects. Mice were euthanized by intracardiac injection of T61 (Merck Animal Health, Kirkland, QC, Canada) under general anesthesia as previously described.[45]

Wholemount Retina Preparation and Immunofluorescence Staining

At the age of 20 weeks, ALS (n = 18, 18F) and control mice (n = 18, 18F) were euthanized by intracardiac injection of T61 (Merck Animal Health, Kirkland, QC, Canada) under general anesthesia as previously described.[45] The eyes were harvested and immersion-fixed in 2% PFA (Electron Microscopy Sciences, Hatfield, PA) at 4 °C for 4 hours. After removal of the cornea, iris, and lens, the retina was detached from the eyecup.[46] The retina was divided into four quadrants with radial cuts and the quadrants were flattened.[47]

Retinas underwent five washes with PBS and then permeabilized by incubation in blocking solution (10% goat serum, 0.3% Triton-X, in 1X PBS) with AffiniPure mouse Fab fragment (30 μg/mL) for 1 hour at room temperature.[48] The retinas were incubated with a primary antibody against phosphorylated neurofilaments (SMI 31, monoclonal mouse IgG1, 1:500; BioLegend, San Diego, CA) for 48 hours at 4 °C. SMI 31 is an axonal marker that is used to identify axonal spheroids in motor neurons[23] and RGC axons in ALS patients.[36] After washes with PBS, the retinas were incubated in

secondary antibodies with Alexa-Fluor 647 goat anti-mouse IgG (H+L) (1:1000; Thermo Fisher Scientific, Waltham, MA) for 2 hours at room temperature. After the final rinse in PBS, the retinas were mounted on slides with the inner surface of the retina facing up using a fluorescent mounting medium (Dako, North America, Inc., Carpinteria, CA). Negative controls were obtained by omitting the primary antibody. The wholemount retinas were imaged using a confocal microscope (LSM900, Zeiss Canada Inc., Toronto, Ontario) with a 63X objective lens (0.5% laser power, 880 gain, z-stacks at 0.2 µm intervals).

Statistical Analysis

The number of puncta at 20 weeks of age in ALS mice was compared with controls using Wilcoxon test. Power analysis of the Wilcoxon Rank Sum Test, used to compare ALS and control mice of the first set of experiments at the age of 20 weeks, was performed using the pwrss package in RStudio (Version 2022.07.1),[49] yielding an 83.9% power (95% Confidence Interval (CI): 80.2%- 87.6%).

The number of IR-puncta in both eyes for each mouse over time was analyzed using a Generalized Linear Mixed-Effect Model (GLMM) using RStudio (Version 2022.07.1).[50] The rate of change between the groups was compared on the log scale using the model. The model incorporated the IR-puncta as the dependent variable and time, genotype, sex, and clinical motor scoring adapted from Hatzipetros et al[40] as independent variables. Power analysis of the GLMM used for the second set of longitudinal experiments was performed using the SIMR package to evaluate the model's ability to detect the main effects,[51] showing an 88% power (95% Confidence Interval (CI): 83.69–93.47) for genotype, 86% power (CI: 82.36–90.28) for time, and 83% power (CI: 78.25–87.58) for sex.

Results

Pathology in the Retinal Nerve Fiber Layer (RNFL)

IR-cSLO was used to image in vivo the fundus of 9-week-old age-matched controls (Figure 1A) and ALS (Figure 1B). IR-cSLO showed hyperreflective profiles in the fundus of ALS mice (Figure 1B). OCT B-scan revealed these profiles were localized to the RNFL (Figure 1C). Henceforth, hyperreflective profiles localized to the RNFL are referred to as IR-puncta. Hyperreflective puncta could not be visualized using BR-cSLO and GR-cSLO AF fundus imaging. In vivo retinal imaging of the first set of experiment at the age of 20 weeks, revealed significantly higher number of IR-puncta in ALS mice (n=8, 4M/4F) compared to controls (n=8, 4M/4F) (2.1 ± 2.3 vs 0.5 ± 0.8, respectively, mean ± SD, $p = 0.036$, Wilcoxon Rank Sum Test) (Figure 2).

Pathology by Age and Sex

Longitudinal in vivo eye imaging was performed at multiple ages, from 9 to 20 weeks, to determine retinal changes over time. Fundus imaging showed that additional ALS IR-puncta appeared over time (Figure 3A). In both control and ALS mice, IR-puncta could be detected in 1 or both eyes. By monitoring the IR-puncta over time, we determined that they were stationary and could be tracked throughout the imaging sessions (Figure 3A and B). In the second set of experiments, at the age of 20 weeks, fundus imaging detected IR-puncta in 15 out of 20 ALS mice and 6 out of 20 control mice. Out of the 20 ALS mice, 14 had a higher count of IR-puncta at 20 weeks compared to 8 weeks of age. In contrast, an increase in the IR-puncta count over the same period was observed in 4 of the 20 control mice. Statistical analysis with GLMM showed that the ALS mutation was significantly associated with IR-puncta development ($p = 0.000232$). Moreover, the increase in the number of IR-puncta in ALS was significantly associated with age ($p = 0.000366$). Slope analysis with GLMM showed that the rate of increase of puncta was significantly different between ALS and control mice (0.17 ± 0.02 vs 0.08 ± 0.03 log number puncta/week, respectively, $p = 0.028$). Furthermore, slope analysis of the longitudinal in vivo retinal imaging showed significant increases in rate of IR-puncta increase in both sexes, when comparing ALS females to control females (0.21 ± 0.04 vs 0.08 ± 0.04 log number puncta/week, respectively, $p = 0.006$) (Figure 4 left panel) and ALS males to control males (0.16 ± 0.04 vs 0.09 ± 0.05 log number puncta/week, respectively, $p = 0.039$) (Figure 4 right panel). In addition, slope analysis with GLMM showed that the increase in IR-puncta over time was significantly steeper in ALS females compared to ALS males (0.21 ± 0.04 vs 0.16 ±

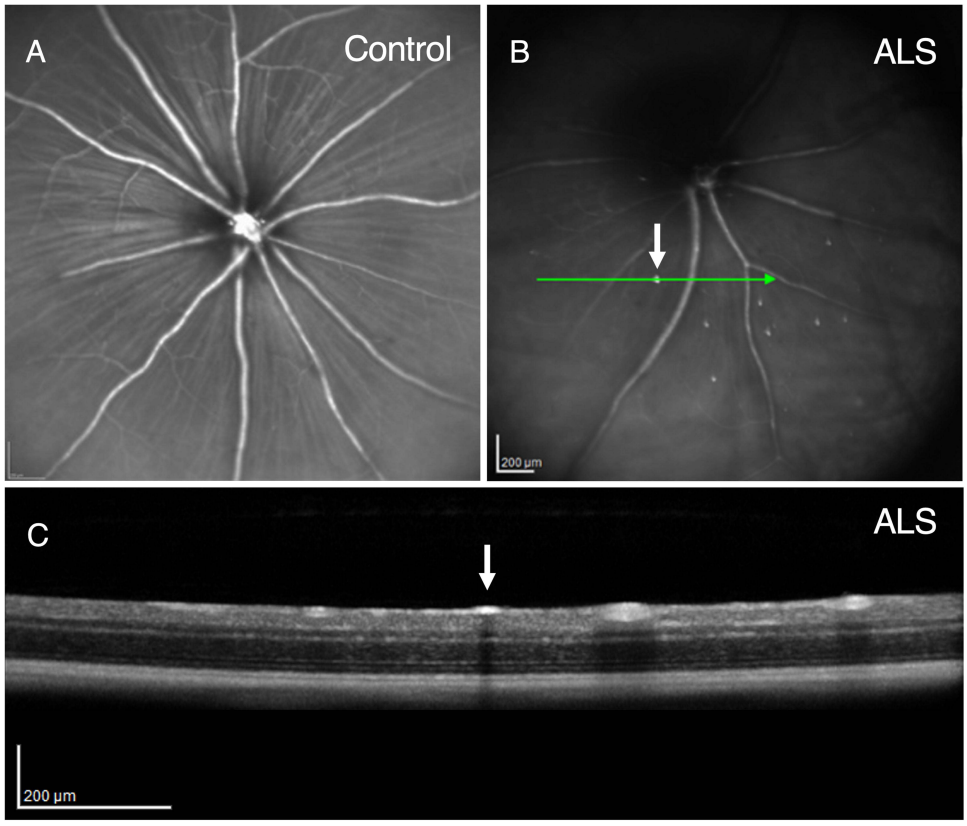

Figure 1 Retinal Pathology in ALS. IR-cSLO imaging of the right fundus of a female mouse at 9 weeks (**A**) showed hyperreflective puncta (**B**). OCT B-scan (green arrow) localized puncta (white arrows) to the retinal nerve fiber layer. Puncta were distinguishable from blood vessels by being more hyperreflective (**C**) Calibration bars, 200 µm. **Abbreviations**: IR, infrared reflectance; cSLO, confocal scanning laser ophthalmoscopy; OCT, optical coherence tomography.

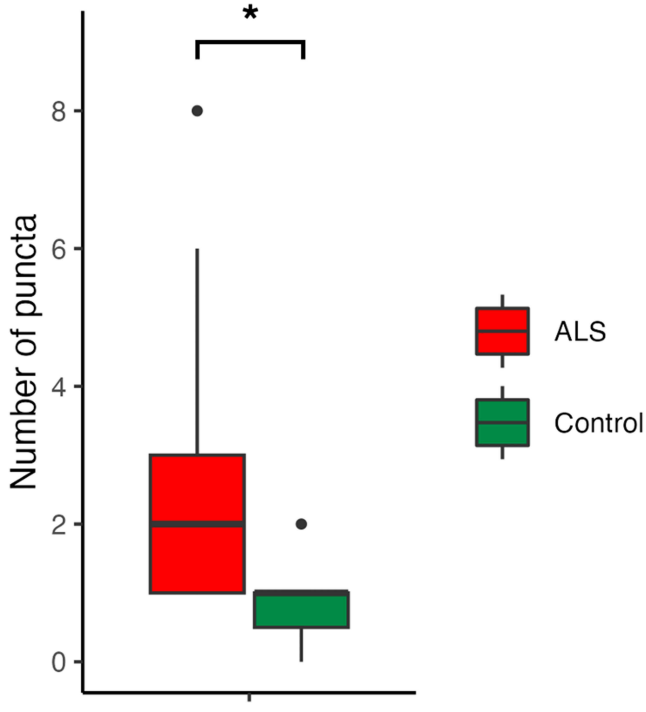

Figure 2 Number of IR-Puncta at 20 weeks. Boxplot of number of puncta at 20 weeks. In the first set of experiments, ALS mice (n = 8, 4M/4F, red) showed significantly more puncta compared to controls (n=8, 4M/4F, green) at 20 weeks (2.1 ± 2.3 vs 0.5 ± 0.8 puncta, respectively, mean ± SD, p = 0.036, Wilcoxon Rank Sum Test). *$p < 0.05$. The horizontal line within each box represents the median; the box shows the interquartile range (IQR); whiskers indicate the range excluding outliers.

https://doi.org/10.2147/EB.S516163

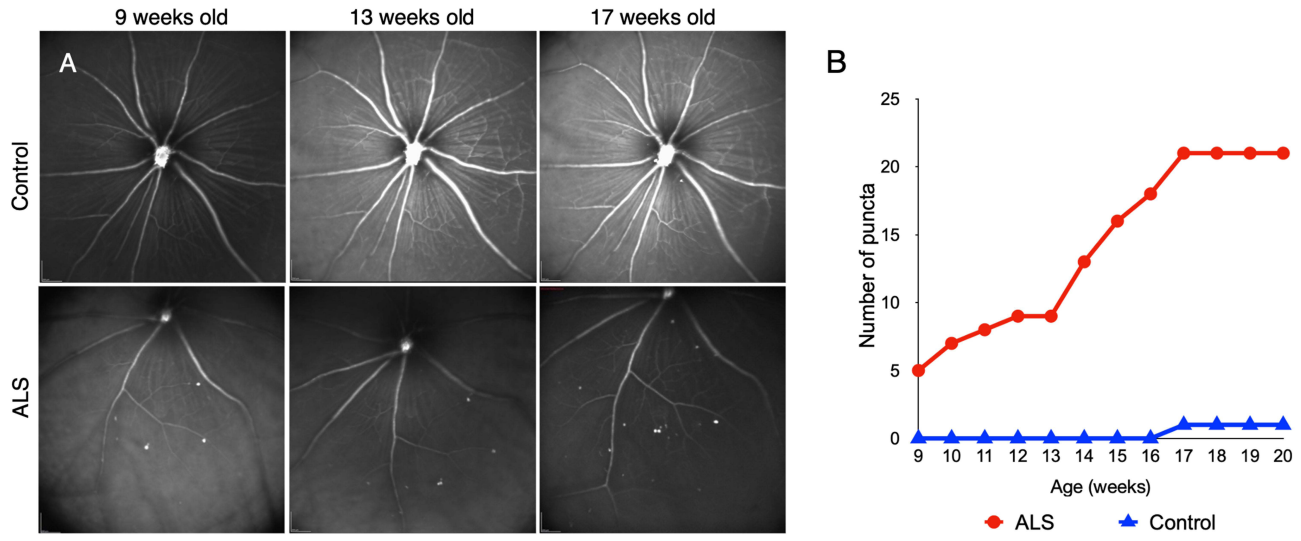

Figure 3 Retinal Pathology with Age. (**A**) Longitudinal IR-cSLO imaging of the left fundus of a female control and ALS mouse at 9, 13, and 17 weeks showed hyperreflective puncta increase in number. (**B**) Plot showing the puncta number of an ALS (red) and control mouse (blue) over time. Calibration bars, 200 µm.
Abbreviations: IR, infrared reflectance; cSLO, confocal scanning laser ophthalmoscopy; RNFL, retinal nerve fiber layer.

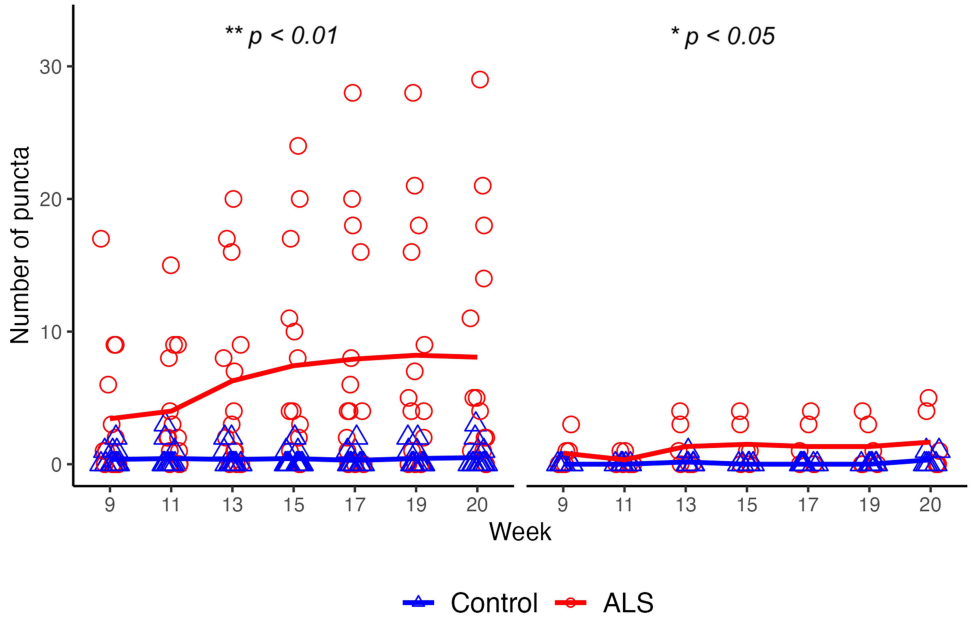

Figure 4 Retinal Pathology by Sex. In the second set of experiments, the rate of puncta increase over time was significant in female ALS (0.21 ± 0.04 vs 0.08 ± 0.04 log number puncta/week, respectively, p = 0.006, left panel) and male ALS mice (0.16 ± 0.04 vs 0.09 ± 0.05 log number puncta/week, respectively, p = 0.039, right panel). Analysis with GLMM revealed that the interaction between genotype and sex over time was significant (p = 0.029). ***p < 0.01, *p < 0.05*.

0.04 log number puncta/week, respectively, p = 0.037). Control females and males showed slopes of 0.08 ± 0.04 and 0.09 ± 0.05, respectively (p = 0.88). The rate of increase of IR-puncta did not correlate with progression of motor signs based on tremor or hindlimb extension reflex assessment (p = 0.071 and p = 0.367, respectively, GLMM).

ALS Axonal Spheroids in RGC Axons

Wholemount retinas of 20-week-old ALS (n = 18, 18F) and control mice (n = 18, 18F) were dissected and immunostained for P-NF, an axonal marker (Figure 5). P-NF immunofluorescence staining revealed RGC axons with a relatively

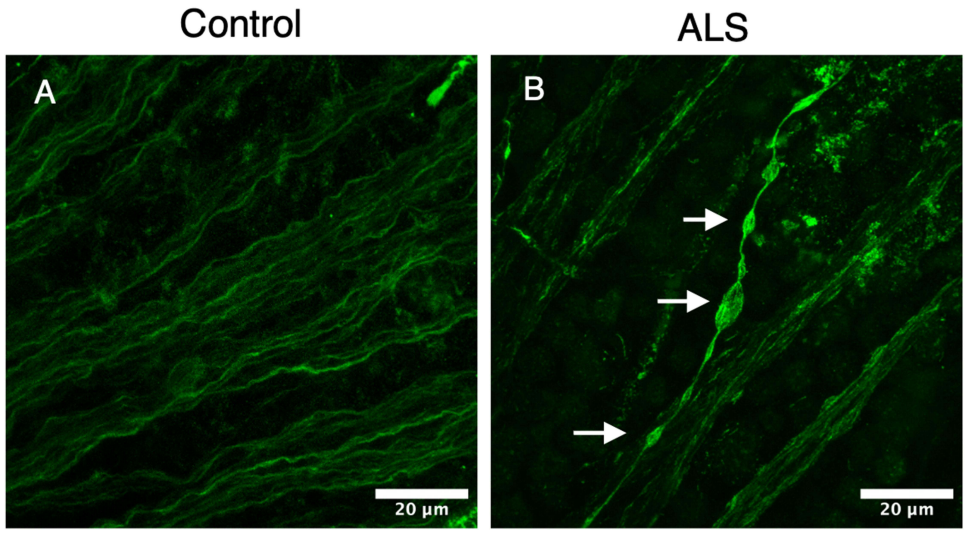

Figure 5 Axonal spheroids in ALS retinal ganglion axons. Immunofluorescence staining for phosphorylated neurofilament (P-NF) of the wholemount retina of a female control mouse at the age of 20 weeks (**A**) showed retinal ganglion cell axons. Wholemount retina of a female ALS mouse at 20 weeks (**B**) showed P-NF+ axonal spheroids (white arrows) in retinal ganglion cell axons in RNFL. P-NF, phosphorylated neurofilament; Calibration bars, 20 µm.

constant thickness along their length in the RNFL (Figure 5A). RGC axons of ALS retinas showed focal thickenings that were positive for P-NF (Figure 5B). In addition, these axons exhibited multiple P-NF-positive axonal spheroids along the same axon (Figure 5B). Accumulation of phosphorylated neurofilament in axonal spheroids, pointed to alteration of axonal transport in the RGCs and axonal pathology.

Discussion

The present study is the first to determine the presence of an in vivo retinal phenotype in the RNFL in a mouse model of ALS. While previous studies have provided insights into changes in thickness of RNFL and retinal vessels in ALS, our identification of discrete hyperreflective puncta within the RNFL represents a novel retinal feature that can be detected and tracked longitudinally in vivo using cSLO coupled with OCT. This finding adds a new dimension to characterize retinal changes in ALS and may offer complementary value to existing structural measures.[28] This longitudinal in vivo eye imaging study showed inner retinal pathology increased with age in ALS mice. Furthermore, females were found to progress faster. We were also able to demonstrate the presence of axonal spheroids in the RGC axons of ALS mice, indicative of axonal transport pathology, as seen in post-mortem retinas of patients with ALS.[36]

Most previous OCT studies in ALS have focused on assessing retinal layer thickness, particularly the RNFL, with mixed findings. Some reported thinning of the macular and peripapillary RNFL in ALS patients,[28–30] with one study noting a correlation between RNFL thinning and clinical severity.[33] However, other studies found no significant differences in RNFL thickness between ALS and control groups.[31,32] Additionally, a small number of studies have described alterations in retinal vasculature, such as increased outer wall thickness of retinal vessels, suggesting broader retinal involvement beyond neural structures.[34] The results of these cross-sectional studies may differ due to ALS phenotypes and disease severity, age, sex, and ethnicityas variations in RNFL thickness among individuals based on age, sex, and race has been described.[52,53] Measurements of the thickness of retinal layers and retinal vessels require manual or computer-based segmentation, which may also be challenging. Furthermore, the number of OCT studies investigating RNFL changes over time is limited. Building upon this body of work, our study identifies discrete hyperreflective puncta in the RNFL—detectable longitudinally in vivo using cSLO combined with OCT—as a novel and progressive retinal feature in ALS. The hyperreflective puncta observed in this study are relatively easier to count and may offer a more accessible and repeatable approach for monitoring retinal phenotypes over time in ALS.

Our study benefits from evaluating IR-puncta longitudinally and demonstrating the progressive nature of this ALS retinal phenotype. The progression of IR-puncta may be a relevant biomarker for assessing retinal phenotype and

https://doi.org/10.2147/EB.S516163

monitoring the progression of ALS patients. This novel approach offers complementary insights beyond layer thickness or vascular morphology and may enhance the resolution at which subtle retinal pathology can be monitored over time.

Although IR-puncta are located in the RNFL that contains the RGC axons, molecular and cellular components forming the ALS IR-puncta are not yet known. Previously, we detected RNFL pathology and presence of neurofilament-positive axonal spheroids in the post-mortem retina of ALS patients.[36] This finding demonstrates that axonal transport pathology in ALS is not limited to motor neurons. In the SOD1 model used in this study, neurofilament-positive axonal spheroids were described in spinal motor neurons.[17,54] Future studies with molecular markers are needed to determine the exact nature of these lesions detectable by imaging.

The sex-dependent progression noted in this study is not inconsistent with reports in which ALS patients showed sex-dependent differences in susceptibility, progression, and motor neuron pathology. For instance, men show higher prevalence, earlier age of onset, and higher white matter tract integrity in the brainstem and cerebellum.[55] Male SOD1G93A mice have elevated aggregation of SOD1 in spinal cord, higher excitotoxicity, and earlier onset of motor symptoms compared to female ALS mice.[56–59] Moreover, female and male mice show different antioxidant response to lipid peroxidation, which is observed in ALS, as they age.[60] In addition, sex hormones seem to have divergent roles in males (detrimental)[61] versus females (protective) as suggested by studies in mouse models of the disease.[8,62–65] Studying the role of sex hormones and other mechanisms underlying sex-dependent differences in the retinal phenotype, along with other phenotypes in ALS mice,[66] may be helpful in understanding the pathobiology of ALS.

The hyperphosphorylation of NFs in ALS is associated with slowed NF transport and leads to axonal transport alteration.[67] Therefore, the presence of P-NF-positive axonal spheroids in the RGC axons suggests that axonal transport alteration in an ALS mouse model can also occur in the long RGC axons in the RNFL. The presence of P-NF-positive axonal spheroids in the retina of SOD1 transgenic mice described in the present study is in keeping with the presence of similar axonal spheroids in the RNFL in post-mortem retina sections from ALS patients.[36] Furthermore, it suggests some of the hyperreflective puncta detected in vivo in the RFNL with cSLO-coupled OCT may correspond to axonal spheroids observed in wholemount ALS retinas.

Other histological changes in the retina of ALS mice have been previously described. A study in the same ALS model described a significant decrease in the total density of Brn3a+ RGCs in 4-month-old SOD1G93A B6.Cg.-Tg(SOD1*G93A) 1Gur/J mice compared to controls.[68] In another ALS mouse model with an ALS-associated mutation of *UBQLN2P497H* gene, ubiquilin2-positive aggregates were detected in the ganglion cell layer, inner plexiform layer, and outer nuclear layer.[30] As specific constituents of IR-puncta are currently unknown, future 3-D correlative histopathological validation studies using other molecular markers for lysosomes and mitochondria, established components of axonal spheroids,[16,22] on serial sections of the retina, are needed to determine the constituents of these hyperreflective puncta in ALS mice.

The limitations of this study include the lack of direct histological validation of the hyperreflective puncta, absence of comprehensive visual and motor assessments, and reliance on a single animal model. While the retinas of mouse models are valuable for studying the retinal changes in ALS, limitations in translatability include thinner retina, and lower number of RGCs compared to human retina.[37,69] Furthermore, *SOD1*, the gene mutated in the mouse model used in this study, represents approximately 2% of the ALS population, warranting additional studies with other common ALS mutations, such as *C9orf72* and *TDP-43*.[9,70,71,] Finally, pilot clinical studies in ALS patients with *SOD1* mutations may be initiated to assess the potential clinical translation.

Another limitation of this work is the absence of functional visual and comprehensive motor assessments. Future studies may incorporate optomotor response[72] and electroretinogram[73] to correlate an increase in puncta with potential visual function changes. Additionally, longitudinal comprehensive motor[56] and cognitive[74] assessments may inform how this progressive retinal phenotype correlates with progression of the disease.[11,13] Inclusion of measures of disease severity may provide additional insight into the relationship between IR-puncta and disease progression, enhancing their potential applicability for clinical studies and trials.

Our findings support the primary objective of identifying a non-invasive biomarker that is progressive and sex-dependent for ALS in a mouse model. Longitudinal eye imaging using cSLO coupled with OCT can supplement existing ocular imaging studies to monitor a retinal phenotype. The ability to detect and monitor this retinal phenotype using FDA-approved, widely available ophthalmic imaging technologies (such as cSLO and OCT) highlights its strong potential for clinical translation. These findings lay the groundwork for future clinical studies aimed at validating retinal hyperreflective puncta as non-invasive biomarkers for

ALS diagnosis, patient stratification, and longitudinal monitoring of disease progression. Moreover, retinal imaging could offer a practical tool for evaluating therapeutic response in ALS clinical trials, complementing existing biomarkers and neurological assessments.

Conclusion

Longitudinal in vivo imaging in ALS mice revealed a discrete retinal biomarker, IR-hyperreflective puncta in the RNFL, that is progressive, and its progression was sex-dependent. Histological evaluation of retina in the ALS mice at the age of 20 weeks also showed P-NF-positive axonal spheroids, similar to those seen in ALS patients[36] suggesting the axonal transport pathology in RGCs in ALS. Despite anatomical differences between species, RGCs are similarly vulnerable to neurodegeneration in both mice and humans, suggesting that these findings could point to shared mechanisms of axonal dysfunction in ALS. Although these results are promising for the development of retinal imaging biomarkers in ALS, their validation in clinical studies in ALS patients is necessary.

Funding

This work was supported by ALS Canada Research Program and Canada Brain Foundation Discovery Grant, Ron and Alayne Metrick Research Fund, Henry S. Farrugia Ophthalmic Research Fund, Dan Sullivan Research Fund, Canada Foundation for Innovation Leaders Opportunity Fund, Canadian Institutes of Health Research, and University Health Network (UHN) Vision Science Research Program.

Disclosure

Dr Yeni Yucel reports lecture fees from Mitsubishi Tanabe Pharma Canada, outside the submitted work. The authors report no other conflicts of interest in this work.

References

1. Hardiman O, Al-Chalabi A, Chio A, et al. Amyotrophic lateral sclerosis. *Nat Rev Dis Primer*. 2017;3(1):17071. doi:10.1038/nrdp.2017.71
2. Tzeplaeff L, Jürs AV, Wohnrade C, Demleitner AF. Unraveling the heterogeneity of ALS—A call to redefine patient stratification for better outcomes in clinical trials. *Cells*. 2024;13(5):452. doi:10.3390/cells13050452
3. Ravits JM, La Spada AR. ALS motor phenotype heterogeneity, focality, and spread. *Neurology*. 2009;73(10):805–811. doi:10.1212/WNL.0b013e3181b6bbbd
4. Crockford C, Newton J, Lonergan K, et al. ALS-specific cognitive and behavior changes associated with advancing disease stage in ALS. *Neurology*. 2018;91(15):e1370. doi:10.1212/WNL.0000000000006317
5. Mehta P, Raymond J, Nair T, et al. Amyotrophic lateral sclerosis estimated prevalence cases from 2022 to 2030, data from the national ALS Registry. *Amyotroph Lateral Scler Front Degener*. 2025:1–6. doi:10.1080/21678421.2024.2447919
6. Chiò A, Calvo A, Ilardi A, et al. Lower serum lipid levels are related to respiratory impairment in patients with ALS. *Neurology*. 2009;73(20):1681–1685. doi:10.1212/WNL.0b013e3181c1df1e
7. Grassano M, Koumantakis E, Manera U, et al. Giving breath to motor neurons: noninvasive mechanical ventilation slows disease progression in amyotrophic lateral sclerosis. *Ann Neurol*. 2024;95(4):817–822. doi:10.1002/ana.26875
8. Jacob SM, Lee S, Kim SH, Sharkey KA, Pfeffer G, Nguyen MD. Brain-body mechanisms contribute to sexual dimorphism in amyotrophic lateral sclerosis. *Nat Rev Neurol*. 2024;20(8):475–494. doi:10.1038/s41582-024-00991-7
9. Gregory JM, Fagegaltier D, Phatnani H, Harms MB. Genetics of amyotrophic lateral sclerosis. *Curr Genet Med Rep*. 2020;8(4):121–131. doi:10.1007/s40142-020-00194-8
10. Rosen DR, Siddique T, Patterson D, et al. Mutations in Cu/Zn superoxide dismutase gene are associated with familial amyotrophic lateral sclerosis. *Nature*. 1993;362(6415):59–62. doi:10.1038/362059a0
11. Cedarbaum JM, Stambler N, Malta E, et al. The ALSFRS-R: a revised ALS functional rating scale that incorporates assessments of respiratory function. BDNF ALS study group (Phase III). *J Neurol Sci*. 1999;169(1–2):13–21. doi:10.1016/s0022-510x(99)00210-5
12. McCombe PA, Pfluger C, Singh P, Lim CYH, Airey C, Henderson RD. Serial measurements of phosphorylated neurofilament-heavy in the serum of subjects with amyotrophic lateral sclerosis. *J Neurol Sci*. 2015;353(1):122–129. doi:10.1016/j.jns.2015.04.032
13. Verde F, Otto M, Silani V. Neurofilament light chain as biomarker for amyotrophic lateral sclerosis and frontotemporal dementia. *Front Neurosci*. 2021;15:679199. doi:10.3389/fnins.2021.679199
14. Foerster BR, Carlos RC, Dwamena BA, et al. Multimodal MRI as a diagnostic biomarker for amyotrophic lateral sclerosis. *Ann Clin Transl Neurol*. 2014;1(2):107. doi:10.1002/acn3.30
15. Bakkar N, Boehringer A, Bowser R. Use of biomarkers in ALS drug development and clinical trials. *Brain Res*. 2015;1607:94–107. doi:10.1016/j.brainres.2014.10.031
16. Sasaki S, Maruyama S, Takeishi M. Observation of the proximal portions of axons of anterior-horn cells in the human spinal cord. *Cells Tissues Organs*. 1990;139(1):26–30. doi:10.1159/000146974

17. Sasaki S, Warita H, Abe K, Iwata M. Impairment of axonal transport in the axon hillock and the initial segment of anterior horn neurons in transgenic mice with a G93A mutant SOD1 gene. *Acta Neuropathol*. 2005;110(1):48–56. doi:10.1007/s00401-005-1021-9
18. Hirokawa N, Sato-Yoshitake R, Yoshida T, Kawashima T. Brain dynein (MAP1C) localizes on both anterogradely and retrogradely transported membranous organelles in vivo. *J Cell Biol*. 1990;111(3):1027–1037. doi:10.1083/jcb.111.3.1027
19. Hirokawa N, Sato-Yoshitake R, Kobayashi N, Pfister KK, Bloom GS, Brady ST. Kinesin associates with anterogradely transported membranous organelles in vivo. *J Cell Biol*. 1991;114(2):295–302. doi:10.1083/jcb.114.2.295
20. Riancho J, Gonzalo I, Ruiz-Soto M, Berciano J. Why do motor neurons degenerate? Actualisation in the pathogenesis of amyotrophic lateral sclerosis. *Neurol Engl Ed*. 2019;34(1):27–37. doi:10.1016/j.nrleng.2015.12.019
21. Carpenter S. Proximal axonal enlargement in motor neuron disease. *Neurology*. 1968;18(9):841–851. doi:10.1212/wnl.18.9.841
22. Hirano A, Donnenfeld H, Sasaki S, Nakano I. Fine structural observations of neurofilamentous changes in amyotrophic lateral sclerosis. *J Neuropathol Exp Neurol*. 1984;43(5):461–470. doi:10.1097/00005072-198409000-00001
23. Munoz DG, Greene C, Perl DP, Selkoe DJ. Accumulation of phosphorylated neurofilaments in anterior horn motoneurons of amyotrophic lateral sclerosis patients. *J Neuropathol Exp Neurol*. 1988;47(1):9–18. doi:10.1097/00005072-198801000-00002
24. Balendra SI, Normando EM, Bloom PA, Cordeiro MF. Advances in retinal ganglion cell imaging. *Eye*. 2015;29(10):1260–1269. doi:10.1038/eye.2015.154
25. Yücel Y, Gupta N. Glaucoma of the brain: a disease model for the study of transsynaptic neural degeneration. In: Nucci C, Cerulli L, Osborne NN, Bagetta G editors. *Progress in Brain Research. Vol 173. Glaucoma: An Open Window to Neurodegeneration and Neuroprotection*. Elsevier; 2008:465–478. doi:10.1016/S0079-6123(08)01132-1
26. Ito YA, Di Polo A. Mitochondrial dynamics, transport, and quality control: a bottleneck for retinal ganglion cell viability in optic neuropathies. *Mitochondrion*. 2017;36:186–192. doi:10.1016/j.mito.2017.08.014
27. Zabel P, Kałużny JJ, Wiłkość-Dębczyńska M, et al. Peripapillary retinal nerve fiber layer thickness in patients with Alzheimer's disease: a comparison of eyes of patients with Alzheimer's disease, primary open-angle glaucoma, and preperimetric glaucoma and healthy controls. *Med Sci Monit Int Med J Exp Clin Res*. 2019;25:1001–1008. doi:10.12659/MSM.914889
28. Khanna RK, Catanese S, Mortemousque G, et al. Exploring amyotrophic lateral sclerosis through the visual system: a systematic review. *Eur J Neurol*. 2024;31(12):e16475. doi:10.1111/ene.16475
29. Rohani M, Meysamie A, Zamani B, Sowlat MM, Akhoundi FH. Reduced retinal nerve fiber layer (RNFL) thickness in ALS patients: a window to disease progression. *J Neurol*. 2018;265(7):1557–1562. doi:10.1007/s00415-018-8863-2
30. Volpe NJ, Simonett J, Fawzi AA, Siddique T. Ophthalmic manifestations of amyotrophic lateral sclerosis (An American ophthalmological society thesis). *Trans Am Ophthalmol Soc*. 2015;113:T12.
31. Roth NM, Saidha S, Zimmermann H, et al. Optical coherence tomography does not support optic nerve involvement in amyotrophic lateral sclerosis. *Eur J Neurol*. 2013;20(8):1170–1176. doi:10.1111/ene.12146
32. Liu Z, Wang H, Fan D, Wang W. Comparison of optical coherence tomography findings and visual field changes in patients with primary open-angle glaucoma and amyotrophic lateral sclerosis. *J Clin Neurosci off J Neurosurg Soc Australas*. 2018;48:233–237. doi:10.1016/j.jocn.2017.10.080
33. Rojas P, de Hoz R, Ramírez AI, et al. Changes in retinal OCT and their correlations with neurological disability in early ALS patients, a follow-up study. *Brain Sci*. 2019;9(12):337. doi:10.3390/brainsci9120337
34. Abdelhak A, Hübers A, Böhm K, Ludolph AC, Kassubek J, Pinkhardt EH. In vivo assessment of retinal vessel pathology in amyotrophic lateral sclerosis. *J Neurol*. 2018;265(4):949–953. doi:10.1007/s00415-018-8787-x
35. Cennamo G, Montorio D, Ausiello FP, et al. Correlation between retinal vascularization and disease aggressiveness in amyotrophic lateral sclerosis. *Biomedicines*. 2022;10(10):2390. doi:10.3390/biomedicines10102390
36. Sharma K, Amin Mohammed Amin M, Gupta N, et al. Retinal spheroids and axon pathology identified in amyotrophic lateral sclerosis. *Invest Ophthalmol Vis Sci*. 2020;61(13):30. doi:10.1167/iovs.61.13.30
37. Huang KC, Tawfik M, Samuel MA. Retinal ganglion cell circuits and glial interactions in humans and mice. *Trends Neurosci*. 2024;47(12):994–1013. doi:10.1016/j.tins.2024.09.010
38. Gurney ME, Pu H, Chiu AY, et al. Motor neuron degeneration in mice that express a human Cu, Zn superoxide dismutase mutation. *Science*. 1994;264(5166):1772–1775. doi:10.1126/science.8209258
39. Acevedo-Arozena A, Kalmar B, Essa S, et al. A comprehensive assessment of the *SOD1G93A* low-copy transgenic mouse, which models human amyotrophic lateral sclerosis. *Dis Model Mech*. 2011;4(5):686–700. doi:10.1242/dmm.007237
40. Hatzipetros T, Kidd JD, Moreno AJ, Thompson K, Gill A, Vieira FG. A quick phenotypic neurological scoring system for evaluating disease progression in the SOD1-G93A mouse model of ALS. *J Vis Exp*. 2015;(104):53257. doi:10.3791/53257
41. Hanna J, Yücel YH, Zhou X, Mathieu E, Paczka-Giorgi LA, Gupta N. Progressive loss of retinal blood vessels in a live model of retinitis pigmentosa. *Can J Ophthalmol*. 2018;53(4):391–401. doi:10.1016/j.jcjo.2017.10.014
42. Liu X, Wang CH, Dai C, Camesa A, Zhang HF, Jiao S. Effect of contact lens on optical coherence tomography imaging of rodent retina. *Curr Eye Res*. 2013;38(12):1235–1240. doi:10.3109/02713683.2013.815218
43. Puk O, Dalke C, Favor J, de Angelis MH, Graw J. Variations of eye size parameters among different strains of mice. *Mamm Genome off J Int Mamm Genome Soc*. 2006;17(8):851–857. doi:10.1007/s00335-006-0019-5
44. Schmucker C, Schaeffel F. In vivo biometry in the mouse eye with low coherence interferometry. *Vision Res*. 2004;44(21):2445–2456. doi:10.1016/j.visres.2004.05.018
45. Hanna J, Yücel YH, Zhou X, Kim N, Irving H, Gupta N. Beta-adrenergic glaucoma drugs reduce lymphatic clearance from the eye: a sequential photoacoustic imaging study. *Exp Eye Res*. 2021;212:108775. doi:10.1016/j.exer.2021.108775
46. Ivanova E, Toychiev AH, Yee CW, Sagdullaev BT. Optimized protocol for retinal wholemount preparation for imaging and immunohistochemistry. *J Vis Exp*. 2013;(82):51018. doi:10.3791/51018
47. Powner MB, Vevis K, McKenzie JAG, Gandhi P, Jadeja S, Fruttiger M. Visualization of gene expression in whole mouse retina by in situ hybridization. *Nat Protoc*. 2012;7(6):1086–1096. doi:10.1038/nprot.2012.050
48. Møllgård K, Beinlich FRM, Kusk P, et al. A mesothelium divides the subarachnoid space into functional compartments. *Science*. 2023;379(6627):84–88. doi:10.1126/science.adc8810

49. Bulus M, Polat C. pwrss R Paketi ile İstatistiksel Güç Analizi. *Ahi Evran Üniversitesi Kirsehir Egitim Fakültesi Derg*. 2023;24(3):2207–2328. doi:10.29299/kefad.1209913
50. Bates D, Mächler M, Bolker B, Walker S. Fitting linear mixed-effects models using lme4. *J Stat Softw*. 2015;67(1). doi:10.18637/jss.v067.i01
51. Green P, MacLeod CJ. SIMR: an R package for power analysis of generalized linear mixed models by simulation. *Methods Ecol Evol*. 2016;7(4):493–498. doi:10.1111/2041-210X.12504
52. Alasil T, Wang K, Keane PA, et al. Analysis of normal retinal nerve fiber layer thickness by age, sex, and race using spectral domain optical coherence tomography. *J Glaucoma*. 2013;22(7):532. doi:10.1097/IJG.0b013e318255bb4a
53. Wu J, Du Y, Lin C, et al. Retinal nerve fibre layer thickness measured with SD-OCT in a population-based study: the Handan eye study. *Br J Ophthalmol*. 2023;107(8):1156–1164. doi:10.1136/bjophthalmol-2021-320618
54. Tu PH, Raju P, Robinson KA, Gurney ME, Trojanowski JQ, Lee VM. Transgenic mice carrying a human mutant superoxide dismutase transgene develop neuronal cytoskeletal pathology resembling human amyotrophic lateral sclerosis lesions. *Proc Natl Acad Sci U S A*. 1996;93(7):3155–3160. doi:10.1073/pnas.93.7.3155
55. Zamani A, Thomas E, Wright DK. Sex biology in amyotrophic lateral sclerosis. *Ageing Res Rev*. 2024;95:102228. doi:10.1016/j.arr.2024.102228
56. Alves CJ, de Santana LP, Dos Santos AJD, et al. Early motor and electrophysiological changes in transgenic mouse model of amyotrophic lateral sclerosis and gender differences on clinical outcome. *Brain Res*. 2011;1394:90–104. doi:10.1016/j.brainres.2011.02.060
57. Molnar-Kasza A, Hinteregger B, Neddens J, Rabl R, Flunkert S, Hutter-Paier B. Evaluation of neuropathological features in the SOD1-G93A low copy number transgenic mouse model of amyotrophic lateral sclerosis. *Front Mol Neurosci*. 2021;14:681868. doi:10.3389/fnmol.2021.681868
58. Herron LR, Miles GB. Gender-specific perturbations in modulatory inputs to motoneurons in a mouse model of amyotrophic lateral sclerosis. *Neuroscience*. 2012;226:313–323. doi:10.1016/j.neuroscience.2012.09.031
59. Veldink JH, Bär PR, Joosten EAJ, Otten M, Wokke JHJ, Van Den Berg LH. Sexual differences in onset of disease and response to exercise in a transgenic model of ALS. *Neuromuscul Disord*. 2003;13(9):737–743. doi:10.1016/S0960-8966(03)00104-4
60. Sobocanec S, Balog T, Kusić B, Sverko V, Sarić A, Marotti T. Differential response to lipid peroxidation in male and female mice with age: correlation of antioxidant enzymes matters. *Biogerontology*. 2008;9(5):335–343. doi:10.1007/s10522-008-9145-7
61. Aggarwal T, Polanco MJ, Scaramuzzino C, et al. Androgens affect muscle, motor neuron, and survival in a mouse model of SOD1-related amyotrophic lateral sclerosis. *Neurobiol Aging*. 2014;35(8):1929–1938. doi:10.1016/j.neurobiolaging.2014.02.004
62. Groeneveld GJ, Van Muiswinkel FL, Sturkenboom JM, Wokke JHJ, Bär PR, Van den Berg LH. Ovariectomy and 17β-estradiol modulate disease progression of a mouse model of ALS. *Brain Res*. 2004;1021(1):128–131. doi:10.1016/j.brainres.2004.06.024
63. Choi CI, Lee YD, Gwag BJ, Cho SI, Kim SS, Suh-Kim H. Effects of estrogen on lifespan and motor functions in female hSOD1 G93A transgenic mice. *J Neurol Sci*. 2008;268(1):40–47. doi:10.1016/j.jns.2007.10.024
64. Kim HJ, Magranè J, Starkov AA, Manfredi G. The mitochondrial calcium regulator cyclophilin D is an essential component of oestrogen-mediated neuroprotection in amyotrophic lateral sclerosis. *Brain*. 2012;135(9):2865–2874. doi:10.1093/brain/aws208
65. Yan L, Liu Y, Sun C, et al. Effects of ovariectomy in an hSOD1-G93A transgenic mouse model of amyotrophic lateral sclerosis (ALS). *Med Sci Monit Int Med J Exp Clin Res*. 2018;24:678–686. doi:10.12659/MSM.908786
66. Heiman-Patterson TD, Deitch JS, Blankenhorn EP, et al. Background and gender effects on survival in the TgN(SOD1-G93A)1Gur mouse model of ALS. *J Neurol Sci*. 2005;236(1):1–7. doi:10.1016/j.jns.2005.02.006
67. Manetto V, Sternberger NH, Perry G, Sternberger LA, Gambetti P. Phosphorylation of neurofilaments is altered in amyotrophic lateral sclerosis. *J Neuropathol Exp Neurol*. 1988;47(6):642–653. doi:10.1097/00005072-198811000-00007
68. Rojas P, Ramírez AI, Cadena M, et al. Retinal ganglion cell loss and microglial activation in a SOD1G93A mouse model of amyotrophic lateral sclerosis. *Int J Mol Sci*. 2021;22(4):1663. doi:10.3390/ijms22041663
69. Grannonico M, Miller DA, Liu M, et al. Comparative in vivo imaging of retinal structures in tree shrews, humans, and mice. *eNeuro*. 2024;11(3):ENEURO.0373–23.2024. doi:10.1523/ENEURO.0373-23.2024
70. Grassano M, Calvo A, Moglia C, et al. Systematic evaluation of genetic mutations in ALS: a population-based study. *J Neurol Neurosurg Psychiatry*. 2022;93(11):1190–1193. doi:10.1136/jnnp-2022-328931
71. Berdyński M, Miszta P, Safranow K, et al. SOD1 mutations associated with amyotrophic lateral sclerosis analysis of variant severity. *Sci Rep*. 2022;12(1):103. doi:10.1038/s41598-021-03891-8
72. Kretschmer F, Sajgo S, Kretschmer V, Badea TC. A system to measure the optokinetic and optomotor response in mice. *J Neurosci Methods*. 2015;256:91–105. doi:10.1016/j.jneumeth.2015.08.007
73. Tomiyama Y, Fujita K, Nishiguchi KM, et al. Measurement of electroretinograms and visually evoked potentials in awake moving mice. *PLoS One*. 2016;11(6):e0156927. doi:10.1371/journal.pone.0156927
74. Kreilaus F, Guerra S, Masanetz R, Menne V, Yerbury J, Karl T. Novel behavioural characteristics of the superoxide dismutase 1 G93A (SOD1) mouse model of amyotrophic lateral sclerosis include sex-dependent phenotypes. *Genes Brain Behav*. 2020;19(2):e12604. doi:10.1111/gbb.12604